MIA analysis of FPGA BPMs and beam optics at APS*

JI Da-Heng(季大恒)[1)] WANG Chun-Xi(王春喜)[2)] QIN Qing(秦庆)

Institute of High Energy Physics, Chinese Academy of Sciences, Beijing 100049, China

Abstract: Model independent analysis, which was developed for high precision and fast beam dynamics analysis, is a promising diagnostic tool for modern accelerators. We implemented a series of methods to analyze the turn-by-turn BPM data. Green's functions corresponding to the local transfer matrix elements R_{12} or R_{34} are extracted from BPM data and fitted with the model lattice using least-square fitting. Here, we report experimental results obtained from analyzing the transverse motion of a beam in the storage ring at the Advanced Photon Source. BPM gains and uncoupled optics parameters are successfully determined. Quadrupole strengths are adjusted for fitting but can not be uniquely determined in general due to an insufficient number of BPMs.

Key words: MIA, PCA, SVD, FPGA BPM, optics parameter, lattice fitting

PACS: 41.85.-p, 29.20.dh, 29.27.Eg **DOI:** 10.1088/1674-1137/36/11/015

1 Introduction

Model independent analysis (MIA) is an emerging spatial-temporal mode analysis technique for beam dynamics study, in which the spatial information comes from a large number of beam position monitors (BPMs) and the temporal information from turn-by-turn beam histories. All the beam histories form a data matrix $\boldsymbol{B} = (b_p^m)\sqrt{P}$ where the column index m indicates the monitor, the row index p the pulse or turn, and P the number of turns. A major method for spatial-temporal mode analysis uses the singular value decomposition (SVD) of $\boldsymbol{B}$ to decompose beam motion into a superposition of orthogonal spatial-temporal modes according to the principal component analysis, which is a major statistical data analysis method [1, 2].

It is important to get reliable beam histories from credible and stable BPMs. The first step in MIA is to identify BPMs with various errors by analyzing

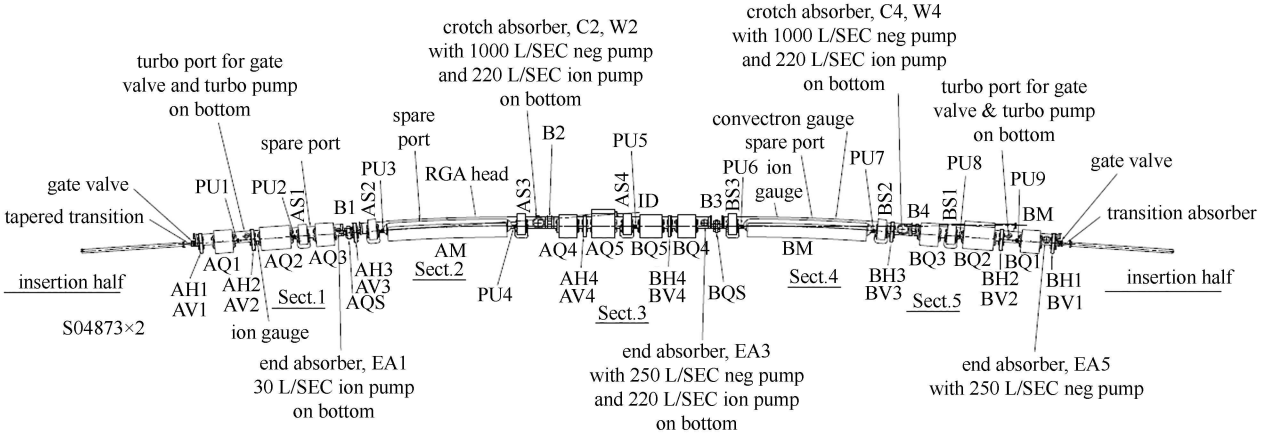

Fig. 1. the arrangement of one of the sectors at the APS storage ring. The BPMs in lattice from sector 29 to sector 40 were replaced by new FPGA BPMs at the time of study.

Received 3 February 2012

* Supported by the Chinese National Foundation of Natural Sciences (111100512108) and National Sciences Foundation of Chinese (10725525)

1) E-mail: jidh@ihep.ac.cn

2) E-mail: wangcx@aps.anl.gov

the turn-by-turn data using different methods and to characterize the used BPM system as much as possible. Although MIA can get much useful information without a lattice model (after all, it was invented for such purposes, as its name suggests), when an adequate model is available, MIA combined with lattice fitting could provide many more results. Thus, in the following treatment, we take the lattice model into account in the MIA calculations. In this paper, we describe our recent effort on BPM system characterization and uncoupled optics function determination.

This study was done at the Advanced Photon Source (APS) storage ring, whose turn-by-turn BPMs are being gradually replaced with new FPGA BPMs. Here we discuss the techniques used to analyze the beam histories from all installed FPGA BPMs. We will first give some results on our evaluation of FPGA BPMs. Then we discuss BPM gain measurement and storage ring optics determination using MIA and lattice fitting.

2 BPM investigation

2.1 FPGA BPMs of APS

The advanced photon source, which is located at Argonne National Laboratory in the US, is a third-generation synchrotron X-ray source that provides intense X-rays for basic and applied research. The storage ring operates at 7 GeV and 100 mA. It has 40 nearly identical sectors. Each includes nine to eleven BPMs. The use of a single FPGA chip to perform the initial signal processing for all analog input channels has a number of advantages over a design using conventional digital signal-processing devices. The chosen FPGA has several multiply accumulate cores, which allows the signal processing for up to eight input channels to be performed on a single chip. This provides increased reliability and reduces power consumption since almost all high-speed signals are contained within that single device and need not pass through I/O pin drivers. These FPGA BPMs can provide 2^{18} turns, about a second long, turn-by-turn beam histories. In the experiment the beam is excited by the feedback system with reverse phase to remove the effect of damping. Overall, the FPGA BPMs supply very valuable data.

2.2 Problematic BPMs

Most of the FPGA BPMs are reliable and their stability is satisfactory. However, several problems still arise during our analysis, as shown in Table 1 and Fig. 2. Some of those in type A and B are simply

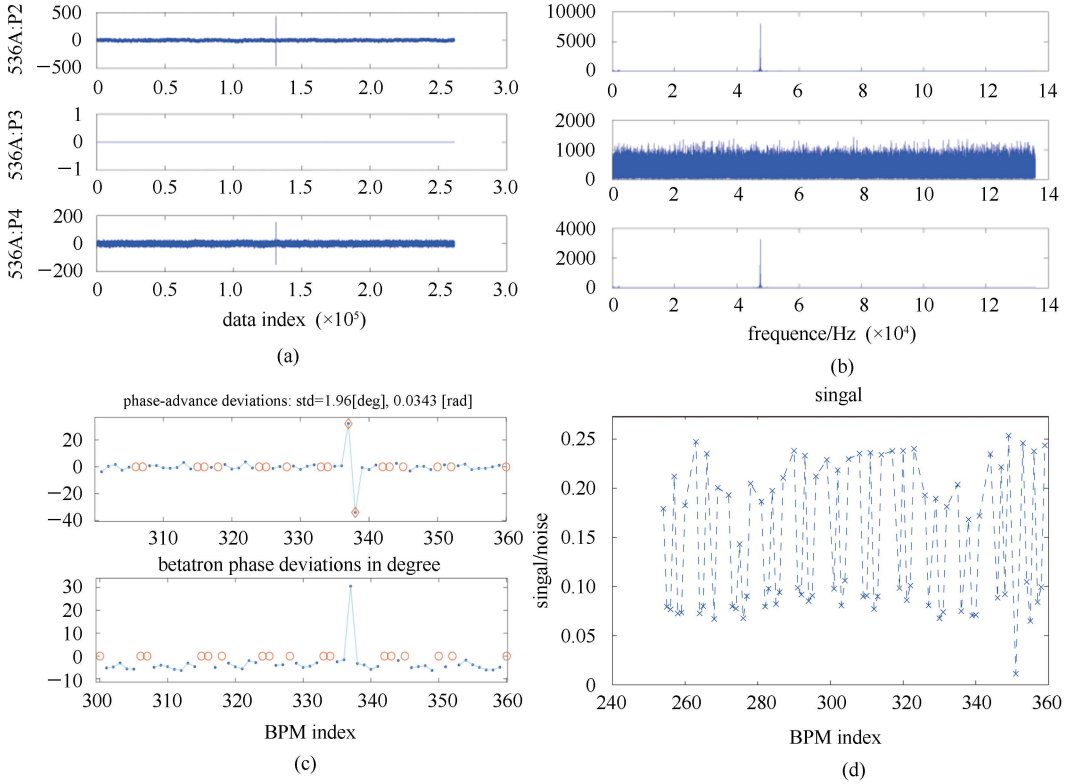

Fig. 2. Illustration of problematic BPMs. (a) Type A, no response signal in the middle BPM; (b) type B, no tune signal in the FFT of the middle BPM; (c) type C, phase-advance error close to tune; (d) type D, unusually low S/N, such as #351.

BPMs used for other purposes. However, there are BPMs with more subtle problems that will be hard to diagnose otherwise. A BPM with a type C problem shows a measured phase advance that differs from the designed value by a multiple of the tune approximately. It is probably caused by turn offsets due to wrong timing, which can often be corrected simply by shifting the beam history. There are also some BPMs that appear to be functioning, but with unusually low signal. Signal strength does vary among BPMs due to beta function and gain setting. However, an unusually low signal-to-noise level indicates problems and including such BPMs in MIA analysis may reduce the overall accuracy of the measured MIA modes [3].

Table 1. Problematic BPMs.

type	behavior	resolution
A	no response signal	removed
B	no tune signal in FFT	removed
C	phase-advance error close to tune	sync data
D	unusually low S/N	removed

2.3 Noise level and its current dependence

BPM noise level is determined by the characteristic noise tail in the singular-value spectrum. To examine the current dependence of BPM resolution, we took beam histories at various currents and the corresponding singular-value spectrum is plotted in Fig. 3. We use the SVD method to decompose the beam history to different modes. The tail of a singular value can present the noise level in signal [4]. Fig. 3 shows the noise level change with beam current. If we take the RMS value of the noise modes, we can get the noise level from different BPMs as shown in Fig. 6.

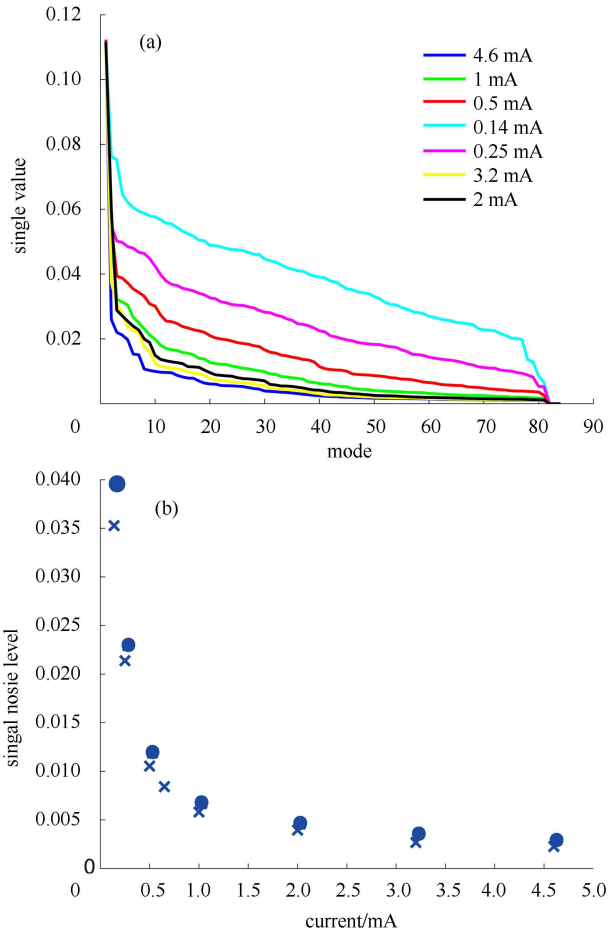

Fig. 3. Noise level and its current dependence. (a) Singular value with current Y plane beam current from up to down: 0.14 mA, 0.25 mA, 0.5 mA, 1 mA, 2 mA,3.2 mA,4.6 mA. (b) Noise level with current. X/Y plane singular value of mode 40. The cross is the X plane and the point is the Y plane.

2.4 Phase-advance measurement accuracy

MIA can be used to measure the tune and phase advance. Fig. 4 shows the tuning accuracy of MIA measurement, which is also compared with the result of FFT. In the figure, the red points represent the tune calculated from beam histories at different BPMs by MIA and the blue curve is the result of the FFT of one beam history.

Ideally, the accuracy of MIA phase measurement is proportional to $1/\sqrt{P}$, where P is the length of beam history [2]. The measured P-dependence is shown in Fig. 5, in which the beam histories of selected length from a single data set are used to compute the uncertainty in phase advance measurement and its dependence on the history length P. It behaves as expected.

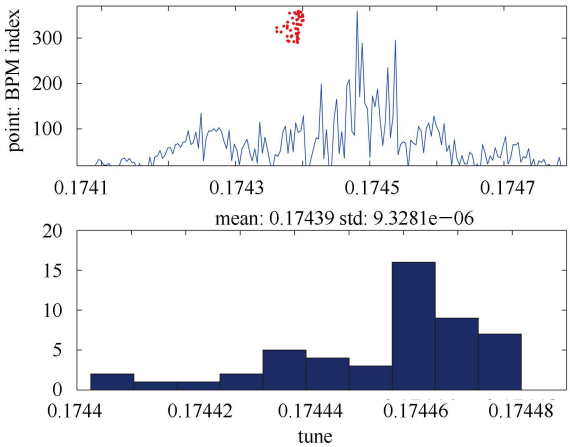

Fig. 4. Up: tune calculation of MIA, compared with the FFT mean. tune: 0.17439, std: 9.3281e −06 down: BPM distribution in tune calculation.

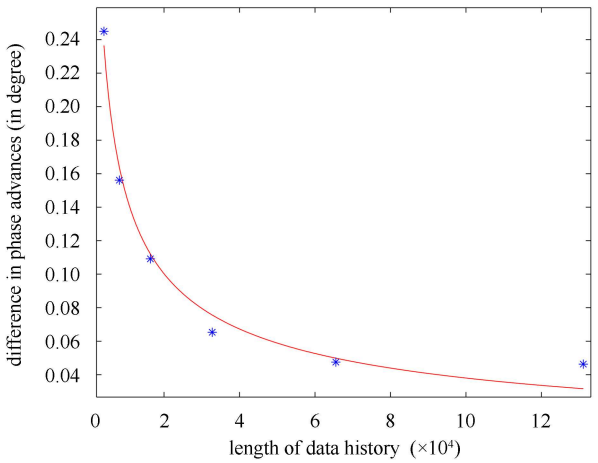

Fig. 5. Phase measurement accuracy verse beam history length. The line is the fitted result with $y=a+b/\sqrt{P}$.

2.5 BPM gains

BPM gain determination relies on beam based measurement and model fitting, which will be discussed in the next section.

2.6 Stability and repeatability

We examined machine stability and measurement repeatability by comparing different measurements under the same conditions. Figs. 6 and 7 contain measurements from three different data sets, shown with different markers. They show excellent repeatability. Note that the tune deviation in Fig. 7 is remarkably small.

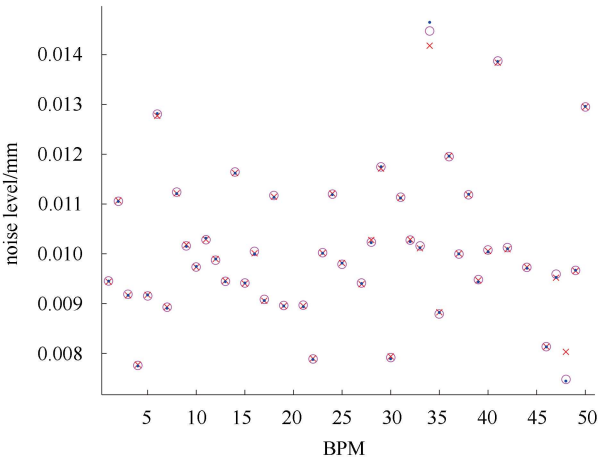

Fig. 6. Noise along BPMs and from different data under the same experimental conditions. Beam current =3.6 mA single bunch. x-axis is BPM order.

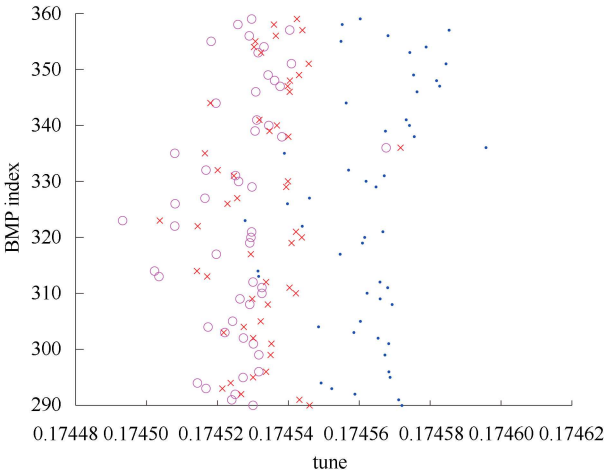

Fig. 7. Tune variation of three data sets measured under the same conditions.

3 Model-independent optics measurement and lattice fitting

3.1 Model-independent optics measurement

An SVD of the beam-history matrix B yields:

$$B=USV^{\mathrm{T}}=\sum\sigma_i\mu_i\upsilon_i^{\mathrm{T}}, \tag{1}$$

where $U_{P\times P}=[\mu_1,\cdots,\mu_P]$ and $V_{M\times M}=[\upsilon_1,\cdots,\upsilon_M]$ are orthogonal matrices containing the temporal vectors μ_i and spatial vectors υ_i. S is a diagonal matrix with nonnegative $\sigma=\sqrt{\lambda}$ along the diagonal in decreasing order. The singular values reveal the number of independent variables and their magnitudes. It can be shown that when beam motion is dominated by betatron oscillation, there are two orthogonal eignmodes (referred to betatron modes) that correspond to the normal coordinates. SVD decomposes the beam history to different modes. More beam facing information can be given by the mean of analyzing these modes. When B is dominated by the excited betatron motion given by $b_p^m=\sqrt{2J_p\beta_m}\cos(\phi_p+\psi_m)$, with action and angle variables independently distributed, it can be decomposed to [5]

$$B\approx\frac{1}{\sqrt{P}}\left(b_p^m\right)=\sigma_+\mu_+\upsilon_+^{\mathrm{T}}+\sigma_-\mu_-\upsilon_-^{\mathrm{T}}, \tag{2}$$

where the spatial and temporal vectors are given by:

$$\begin{cases}\mu_+=\left\{\sqrt{\dfrac{2J_p}{P\langle J\rangle}}\cos(\phi_p-\phi_0),\ p=1,\cdots,P\right\},\\ \mu_-=\left\{\sqrt{\dfrac{2J_p}{P\langle J\rangle}}\sin(\phi_p-\phi_0),\ p=1,\cdots,P\right\},\end{cases} \tag{3}$$

and

$$\begin{cases} \upsilon_+ = \dfrac{1}{\sqrt{\lambda_+}}\left\{\sqrt{\langle J\rangle\beta_m}\cos(\phi_0+\psi_m),\ m=1,\cdots,M\right\}, \\ \upsilon_- = \dfrac{1}{\sqrt{\lambda_-}}\left\{\sqrt{\langle J\rangle\beta_m}\sin(\phi_0+\psi_m),\ m=1,\cdots,M\right\}. \end{cases} \tag{4}$$

From the spatial vector we can get

$$\psi = \tan^{-1}\left(\frac{\sigma_-\upsilon_-}{\sigma_+\upsilon_+}\right), \tag{5}$$

$$\beta = \langle J\rangle^{-1}(\lambda_+\upsilon_+^2+\lambda_-\upsilon_-^2). \tag{6}$$

The reference point of phase does not matter in phase-advanced calculation. So the phase advance and beta function can be obtained from the spatial vector directly. In practice, BPM gains have to be taken into account. The phase measurement is not affected by the BPM gains and is independent of the lattice model. The standard deviation of the measured phase advance from the default lattice is about 2° in our experiments, which is much worse than the phase measurement accuracy. Thus, such a phase-advance measurement can provide valuable information for optics correction. On the other hand, beta-function measurement depends on the BPM gains. Given a good model of the lattice, we can fit the data and lattice model to determine the BPM gains. The results of beta measurement, with and without BPM-gain correction, are shown in Fig. 8. We see that it is critical to measure the BPM gains, which will be addressed in the next section.

3.2 Lattice fitting

Since FPGA BPMs were installed on only about a third of the ring at the time of this study, we need local quantities as the fitting targets. Note that beta functions and phase advances are global quantities that can be changed by magnets far from the BPMs used in the measurement. We choose the R_{12} element of the transfer matrix for fitting, which is affected only by the local magnet strengths, and given by [6]

$$M(s_2|s_1) = \begin{pmatrix} \cdots & R_{12} \\ \cdots & \cdots \end{pmatrix}, \tag{7}$$

and

$$\begin{aligned} R_{12} &= \sqrt{\beta_1\beta_2}\sin(\psi_2-\psi_1) \\ &= \sqrt{\beta_2}\sin(\phi_0+\psi_2)\sqrt{\beta_1}\cos(\phi_0+\psi_1) \\ &\quad -\sqrt{\beta_2}\cos(\phi_0+\psi_2)\sqrt{\beta_1}\sin(\phi_0+\psi_1), \end{aligned} \tag{8}$$

where β_1, ψ_1 is beta function and phase at s_1, β_2, ψ_2 is beta function and phase at s_2. Inserting the measured betatron mode in Eq. (4) into Eq. (8) we get

$$R_{12ij}^{\rm data} = \frac{1}{\langle J\rangle}(\sigma_+\upsilon_{+j}\sigma_-\upsilon_{-i}-\sigma_-\upsilon_{-j}\sigma_+\upsilon_{+i}). \tag{9}$$

Taking the BPM gains into account, we have

$$R_{12ij}^{\rm data} = \frac{1}{\langle Jg_ig_j\rangle}(\sigma_+\upsilon_{+j}\sigma_-\upsilon_{-i}-\sigma_-\upsilon_{-j}\sigma_+\upsilon_{+i}) \tag{10}$$

and

$$(X_{\rm quad,bpm,etc})^{\rm T} = (\Delta R_{12})/(\partial R_{12}/\partial X_{\rm quad,bpm,etc}). \tag{11}$$

where X contains the lattice parameters used for fitting. Here ΔR_{12} is fixed by lattice parameters. If the number of lattice parameters is more than the number of the equation's rank, ΔR_{12} can be uniquely determined.

The number of BPM gains must be less than the number of the equation's rank because of $\mathrm{Rank}_{R_{12}} \approx 2\times\mathrm{NUM_{BPM}}$. So the BPM gains could be uniquely determined.

$$(G_{\rm bpm})^{\rm T} = (\Delta R_{12})/(\partial R_{12}/\partial G_{\rm bpm}). \tag{12}$$

To confirm our BPM-gain measurement, we changed the gain of the BPM S39A:P2 from 1.2367 to 1 and the gain of BPM S35A:P2 from 1.2357 to 1, then repeated the measurement. The difference in the measured gains is shown in Fig. 9. It demonstrates that the measurement results reflect the actual BPM gains. The difference between measured and set values are about 0.5%. Taking the gains into account, the result of beta calculation in Fig. 8(b) is much closer to default lattice than Fig. 8(a).

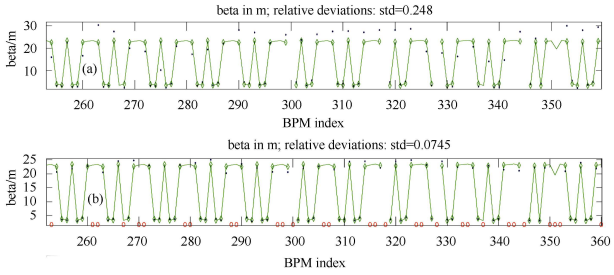

Fig. 8. Result of beta-function measurement with and without BPM-gain correction. Points are measured beta, diamonds are modeled beta, and circles are unavailable BPMs. (a) without gain, std: 0.248; (b) with gain, std: 0.0745.

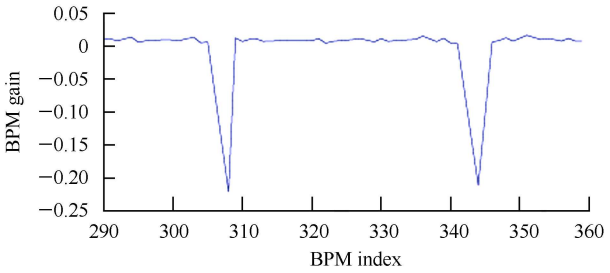

Fig. 9. Deviation of fitting. Two BPMs gains were changed.

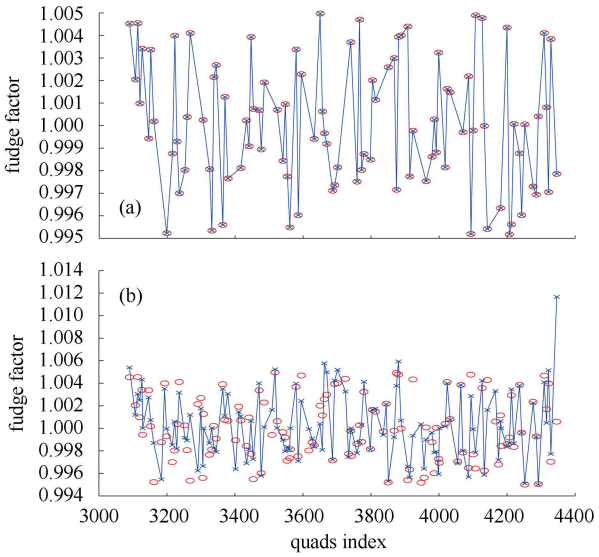

Fig. 10. Quad fitting result. (simulation) Circle is the set value. Cross is the fitting result. The quad number between each two neighbor BPM in (a) is less than 2 and in (b) is not limited.

Quadrupole strengths were also done in our calculation. The betatron modes of each BPM provide two freedoms in each plane. For each plane, fitting BPM gain will take one freedom. If the number of quadrupole magnets between two adjacent BPMs is less than 2, we can get exact solutions. Otherwise, approximate solutions of quad strengths would be given. For both planes each BPM provides four fitting freedoms. BPM gain fitting will take up two. So we can accurately determine two lattice parameters between two BPMs. If the number of quadrupoles between two BPMs is more than two, the quadrupole strength cannot be uniquely determined as shown in Fig. 10.

But in Y plane, the measurement result is much worse than that in the X plane. So fitting of both planes does not work well. Now we suspect that the wake field, transverse coupling, or the sextupole offsets affect the beam measurement, since they are not yet considered in our model.

4 Conclusion and discussion

We evaluated the FPGA BPM system using MIA and developed the MIA-based optics fitting programs for APS optics measurement and lattice fitting, assuming negligible coupling for now. As expected, MIA is proved to be an effective method for beam optics measurement of the APS storage ring. The FPGA BPMs provide second-long beam histories, which can be very powerful for improving the accuracy of beam parameter measurement with MIA. The accuracy of the phase advance measurement is remarkably good (better than 0.1 degree in some cases) and independent of the machine lattice model. Since the beta function measurement needs BPM gains, we developed the BPM gain and quadrupole strength fitting programs in MATLAB. Despite some limitations in optics fitting, BPM gains can be reliably determined by fitting the measurement results with the machine model. Thus, beta functions can be measured rather accurately (better than 1% relative error).

Limited by an insufficient number of BPMs, quadrupole strength errors cannot be uniquely determined, even in the simulations. We found that, unlike many other machines, wake field plays a significant role in the optics seen by the beam, whose effect is yet to be taken into account in our model fitting. We also have not taken into account the transverse coupling and sextupole offsets. Due to these limitations, the lattice fitting is not satisfactory at the moment and needs to be improved in further studies.

References

1 Irwin J, WANG C X, YAN Y et al. Phys. Rev. Lett., 1999, **82**(8): 1684
2 WANG Chun-Xi. Model Independent Analysis of Beam Centroid Dynamics in Accelerators. Ph.D. dissertation, Stanford University, 1999. Also available as SLAC-R-547
3 WANG C X, Borland M, Sajaev V, Kim K. BPM System Evaluation Using Model Independent Analysis. PAC2001, 2001, 1354
4 WANG Chun-Xi, John Irwin, Karl Bane, CAI Yun-Hai, Michiko Minty, Franz J. Decker, YAN Yi-Ton. SLAC-PUB-7909, 1999
5 WANG Chun-Xi. Phys. Rev. ST Accel. Beams, 2003, **6**: 104001
6 WANG Chun-Xi. Measurement and Application of Betatron Modes with MIA. Particle Accelerator Conference, 2003